Edelweiss Applied Science and Technology
ISSN: 2576-8484
Vol. 10, No. 5, 238-256
2026
Publisher: Learning Gate
DOI: 10.55214/2576-8484.v10i5.12913

Microbicidal potential of mercaptopropionic acid-capped cadmium telluride quantum dots against bacteria at varying reflux times

Ezinne U. Ekwujuru[1*], Michael J. Klink[2], Mzimkhulu E Monapathi[1]
[1,3]Department of Natural Sciences, Vaal University of Technology, Vanderbijlpark Campus,1900, South Africa; ezinneekwujuru@yahoo.com (E.U.E.) mzimkhulum@vut.ac.za (M.E.M.).
[2]Department of Chemistry, College of Science, Engineering and Technology, Florida Science Campus, University of South Africa, Roodepoort 1709, South Africa; klinkmj@unisa.ac.za (M.J.K.).

Abstract: Antimicrobial resistance to conventional antibiotics remains a critical global problem, necessitating the development of alternative therapeutic agents such as cadmium telluride quantum dots (CdTe QDs), which exhibit diverse biocidal activity due to their nanoscale dimensions and enhanced free radical generation. This study focused on the synthesis, characterization, and evaluation of the antimicrobial activity of mercaptopropionic acid-capped CdTe QDs (mCdTe QDs) at varying reflux times (1, 2, and 3 hours). The QDs were synthesized using a colloidal chemistry approach. Characterization was performed using Transmission Electron Microscopy (TEM), Scanning Electron Microscopy (SEM), Fourier Transform Infrared Spectroscopy (FTIR), X-ray Diffraction (XRD), and Energy-Dispersive X-ray (EDX). Antimicrobial activity was assessed using agar well diffusion, minimum inhibitory concentration (MIC), and minimum bactericidal concentration (MBC) assays against Escherichia coli and Staphylococcus aureus. XRD analysis confirmed the hexagonal crystalline structure of the QDs, while SEM and TEM revealed uniform particles with average sizes of 3.029 nm, 2.656 nm, and 5.002 nm for 1-hour, 2-hour, and 3-hour reflux durations, respectively. A dose-dependent antimicrobial response was observed, with the 2-hour refluxed sample showing the highest bactericidal activity. Overall, mCdTe QDs exhibited higher efficacy against E. coli than S. aureus, highlighting their potential as effective antimicrobial agents.

Keywords: *Antimicrobial, Bactericidal, Cadmium telluride, Nanotechnology, Quantum dots, Reflux time.*

1. Introduction

Pathogenic microorganisms can cause serious health issues, especially in immunocompromised people [1]. Examples of such organisms include *Staphylococcus aureus* and *Escherichia coli* [2]. Their activity is controlled with conventional antibiotics, but increasing antimicrobial resistance [3, 4] affects their effectiveness. This resistance has raised the prevalence of microbial infections, leading to higher mortality and morbidity rates [5]. Consequently, there is a continuous search for effective alternative antimicrobial agents [3, 4].

Quantum dots (QDs), also known as semiconductor nanocrystals, are among the most fascinating materials in nanotechnology. They are ultra-small, usually ranging between 1.5 to 10.0 nm [6]. They have unique physicochemical properties as a result of their quantum confinement effects [7]. They also demonstrate size- and composition-dependent optoelectronic characteristics with excellent structural stability [5, 6]. QDs are commonly employed in biosensing, imaging, multicolor labeling, real-time tracking, drug delivery, and biological applications [5, 8, 9]. More recently, their potential as antimicrobial agents has captured researchers' interest. This interest is largely attributed to their high electron transfer capabilities, which facilitate the production of free electrons and holes, resulting in a significant pile-up of free radicals [5].

History: Received: 18 March 2026; Revised: 1 May 2026; Accepted: 5 May 2026; Published: 21 May 2026
* Correspondence: ezinneekwujuru@yahoo.com

Among the quantum dots, cadmium telluride (CdTe) quantum dots are of particular interest due to their compatibility with solution-based processes, tunable photoluminescence, and high photostability [10]. CdTe QDs are toxic to human cells [5, 11], though their toxicity level depends greatly on the concentration [5]. Strategies such as coating with poly-L-lysine [5], surface modification using certain capping ligands [8], biosynthesis [12], and encapsulation [13] CdTe QDs have been able to be made more biocompatible.

CdTe quantum dots have shown promise as effective microbicidal agents. For instance, Kumari et al. used CdTe QDs against soil-isolated *Bacillus subtilis*, which demonstrated high bactericidal activity [14]. More interestingly, Wansapura and his group utilized chitin-coated CdTe QDs as antibacterial agents against *Staphylococcus aureus* and *Pseudomonas aeruginosa* [15]. The biohybrid exhibited excellent antibacterial activity against both microorganisms. CdTe QDs were also used against *Porphyromonas gingivalis*, yielding good results, with better performance after laser diode 940-nm irradiation [16]. The bactericidal activities of CdTe QDs depend on their ability to generate reactive oxygen species (ROS) and destroy bacterial membranes [5]. The bactericidal abilities are highly affected by factors such as quantum dot size, surface chemistry, and synthesis conditions, including refluxing time during nanomaterial preparation [17].

Refluxing time is a critical parameter in the production of CdTe QDs. It affects their size, crystallinity, and surface properties, which in turn influence their interaction with bacterial cells [18, 19]. For instance, prolonged refluxing times can result in larger QDs with reduced surface energy, limiting ROS production [20, 21]. Conversely, shorter refluxing times may produce smaller QDs with higher surface energy and enhanced interaction with bacterial cells, increasing their microbicidal activity [22, 23]. Therefore, understanding the effect of refluxing time on the antimicrobial efficacy of CdTe QDs is important.

The present study aimed to investigate the microbicidal potential of CdTe QDs synthesized at different refluxing times against selected bacterial species. By demonstrating how refluxing time affects the size, surface properties, and antimicrobial activity of these QDs, this research explored the potential use of CdTe QDs as alternative antibacterial agents. Findings from the study could strengthen the urgency to find new strategies in fighting resistant bacteria and highlight the impact of nanotechnology on antimicrobial research.

2. Materials and instrumentation

2.1. Materials

The following materials: Tellurium powder, 3-mercaptopropionic acid (MPA), cadmium chloride, NaOH, and ethanol (99.98%) were sourced from Glassworld, Johannesburg, South Africa, and used as purchased without any further purification.

2.2. Instrumentation

X-ray diffraction patterns of the synthesized mCdTe QDs were studied using the Malvern Panalytical Empyrean X-ray diffractometer (Malvern Panalytical, Almelo, Netherlands) with Cu-Kα radiation (λ = 1.54060 Å) under a voltage of 40 kV and 40 mA current. Phase identification was performed with X'Pert HighScore Plus software, version 2.0. FTIR spectra were obtained using a Nicolet iS50 FTIR Spectrometer (Thermo Fisher Scientific, WI, USA). SEM micrographs were captured with a Vega 3 Model No. 2011, TESCAN, Brno, Czech Republic, at an accelerating voltage of 20 kV. An energy-dispersive X-ray (EDX) spectrometer (Oxford Instruments, X-Max, Abingdon, UK), attached to the SEM, was used for elemental analysis of the QDs. TEM analysis was conducted with a JEOL transmission electron microscope, model JEM-2100, Tokyo, Japan, operating at 200 kV accelerating voltage and a beam current of approximately 107 μA.

Edelweiss Applied Science and Technology
ISSN: 2576-8484
Vol. 10, No. 5: 238-256, 2026
DOI: 10.55214/2576-8484.v10i5.12913

3. Experimental Procedure

3.1. Production of MPA-capped CdTe QDs (mCdTe QDs)

The colloidal chemistry technique described in the literature [24] was used with minor modifications. In brief, 0.069 g of $CdCl_2$ was dissolved in 25 mL of distilled water, followed by injection of 55 µL of 3-mercaptopropionic acid (MPA) and 30-minute deaeration with nitrogen gas. Subsequently, the oxygen-free NaHTe solution, produced separately by reacting 0.3 g $NaBH_4$ (in 25 mL of water at 60 °C) with 0.016 g tellurium powder, was added under vigorous stirring. This experiment was performed in triplicate. The solutions were then refluxed at 100 °C for 1 h, 2 h, and 3 h, respectively. The solutions were precipitated using one volume of absolute ethanol and allowed to stay undisturbed for 24 h at 4 °C before centrifugation for 30 min to obtain mCdTe QDs. The precipitate was dried at room temperature and stored in the dark at 4 °C to maintain its integrity [25].

3.2. Antibacterial activity of the synthesized mCdTe QDs

Agar well diffusion method [26], minimum inhibitory concentration (MIC) assay [26], and minimum bactericidal concentration (MBC) test [27] were employed to assess the antimicrobial activities of the mCdTe QDs refluxed at 1, 2, and 3 hours, at concentrations of 10, 50, and 100 mg/mL against *Staphylococcus aureus* (ATCC 25923) and *Escherichia coli* (ATCC 25922), supplied by the Microbiology Laboratory, Vaal University of Technology, South Africa. A loopful of the pure bacterial strain was inoculated into Mueller-Hinton (MH) broth (BioLab Merck, Darmstadt, Germany) and incubated overnight at 37°C in a rotary shaker set at 160 rpm to reach a concentration of colony-forming units (CFU) of ~ 10^6 per millilitre (CFU/mL).

3.2.1. Antibacterial activity by the agar well diffusion method

Susceptibility of the test bacteria against CdTe QDs was evaluated at various doses (10, 50, and 100 mg/ml) and refluxing times (1, 2, and 3 h) using a modified method described in literature [28]. In brief, an overnight culture (100 µL) was evenly spread onto an MH agar (BioLab Merck, Darmstadt, Germany) plate with the aid of a sterile cotton swab. The plates were allowed to dry for 2 min. Holes of about 5 mm in diameter were bored on the inoculated agar plate using the head of a sterile 200 µL micropipette tip. About 30 µL of the test samples were deposited into their respective holes. The positive control (neomycin; 50 mg/mL) and negative control (sterile distilled water) were also loaded into their respective holes. The plates were sealed with parafilm and incubated at 37 °C for 24 h. The experiments were carried out in triplicate. The diameter of the clear zones (zones of inhibition) around the wells was measured in millimeters with a ruler and recorded.

3.2.2. Minimum Inhibitory Concentration (MIC) Test

Sterile 96-well microtiter plates were used in this test to determine the inhibitory potentials of the synthesized mCdTe QD samples. The bacterial culture used was prepared as follows: about 9 mL of sterile MH broth was pipetted into three different test tubes. Then 1 mL of the overnight culture was transferred into the first test tube, followed by serial dilutions up to a 10^{-3} dilution factor, which was used for the MIC test. About 100 µL of the 10^{-3} dilution factor bacterial culture was injected into all the wells using a multichannel pipette, followed by the addition of 50 µL of mCdTe QDs samples, neomycin, and distilled water into the first row of their respective wells in duplicate. A two-fold serial dilution was carried out down the rows. The plates were sealed with parafilm and incubated at 37 °C for 24 hours. The parafilm prevented evaporation, contamination, and cross-contamination between wells [29, 30]. At the end of incubation, about 30 µL of 0.02% resazurin dye was added to all the wells, followed by an overnight incubation. Colour changes were observed. The wells that retained the blue colour of the dye were noted, and the MIC values recorded.

Edelweiss Applied Science and Technology
ISSN: 2576-8484
Vol. 10, No. 5: 238-256, 2026
DOI: 10.55214/2576-8484.v10i5.12913

3.2.3. Minimum Bactericidal Concentration (MBC) Test

MBC is used to complement MIC results by checking the lethality of the samples [31]. The wells that retained the blue color of the dye in the MIC experiment were further investigated to determine the type of antibacterial activity (bacteriostatic or bactericidal) that occurred at various MIC values. Bacterial suspension from these wells was subcultured by dropping about 50 µL onto MH agar plates and spreading them with a sterile cotton swab. The experiments were performed in triplicate. Plates were incubated for 24 hours at 37°C. The lowest concentration with no bacterial growth was considered the MBC [27].

4. Results and Discussion

4.1. Characterization of Nanoparticles

4.1.1. Fourier Transform Infrared (FTIR) Spectroscopy Analysis

The FTIR spectra of the prepared MPA-capped CdTe QDs at different reflux times are presented in Figure 1. The characteristic thiol (S–H) stretching vibration of the capping agent (3-mercaptopropionic acid), typically observed around 2643.5 cm^{-1}, is absent, suggesting effective covalent attachment of the thiol to the QD surface [32]. The IR band at around 3346.5 cm^{-1} represents the stretching vibrations of the O-H from adsorbed water molecules on the surface of the QDs [33] and also indicates effective binding of the capping agent [34]. The bands at 1341, 1128.4, 995.4, and 822.9 cm^{-1} correspond to C-H bending, C-O stretching vibrations, C-H in-plane bending, and C-O-O vibrations, respectively, arising from the capping agent [34, 35]. The vibrational band around 701.6 cm^{-1} is assigned to Cd-Te stretching, confirming the successful formation of CdTe QDs [36]. Similar vibrational bands were observed in other studies [37, 38].

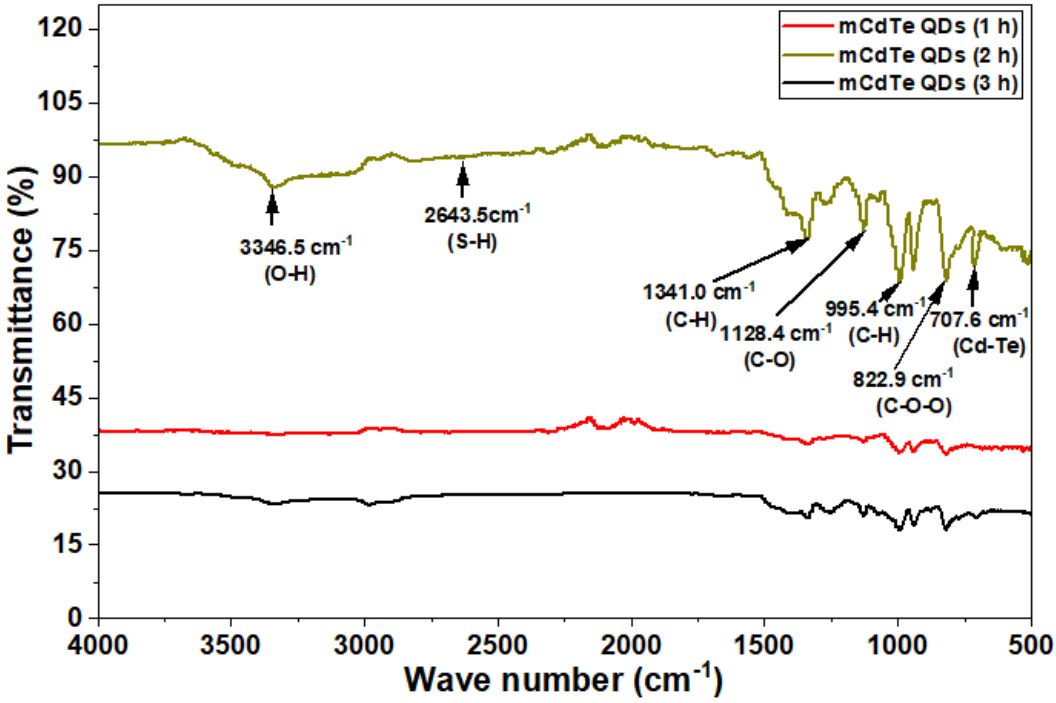

Figure 1.
FTIR spectra of MPA-capped CdTe QDs at reflux times of 1, 2, and 3 h.

Edelweiss Applied Science and Technology
ISSN: 2576-8484
Vol. 10, No. 5: 238-256, 2026
DOI: 10.55214/2576-8484.v10i5.12913

4.1.2. X-ray Diffraction (XRD) Analysis

The XRD patterns of mCdTe QDs synthesized at reflux times of 1, 2, and 3 hours are presented in Figure 2a. Distinct diffraction peaks are observed at 2θ values of 23.6, 25.7, 26.4, 30.2, 34.8, 41.1, 45.2, 49.3, and 50.6, which correspond to the Miller indices (100), (101), (003), (102), (013), (110), (112), (201), and (015), respectively, in all samples, indicating a similar crystal phase. These crystallographic planes confirm the formation of crystalline QDs with a hexagonal structure, as identified using the Joint Committee on Powder Diffraction Standards (JCPDS) card number 04-006-7486 (Figure 2b). The results align with findings in the literature [39, 40]. The sample refluxed for 3 hours exhibited the highest and sharpest peak, suggesting an improvement in crystallinity, increased crystallite size, and a more ordered structure due to extended reflux time. The 1-hour sample showed reduced peak intensity, while the 2-hour sample exhibited the weakest peaks among the three, indicating lesser crystallinity, smaller crystallite sizes, and higher structural disorder [41]. This correlates with the average particle size results (Figures 4d-f), where the 3-hour sample has the largest size and the 2-hour sample the smallest. Overall, the XRD results suggest that reflux time significantly influences the crystallinity and structural integrity of the QDs, with longer reflux durations producing better-ordered crystals.

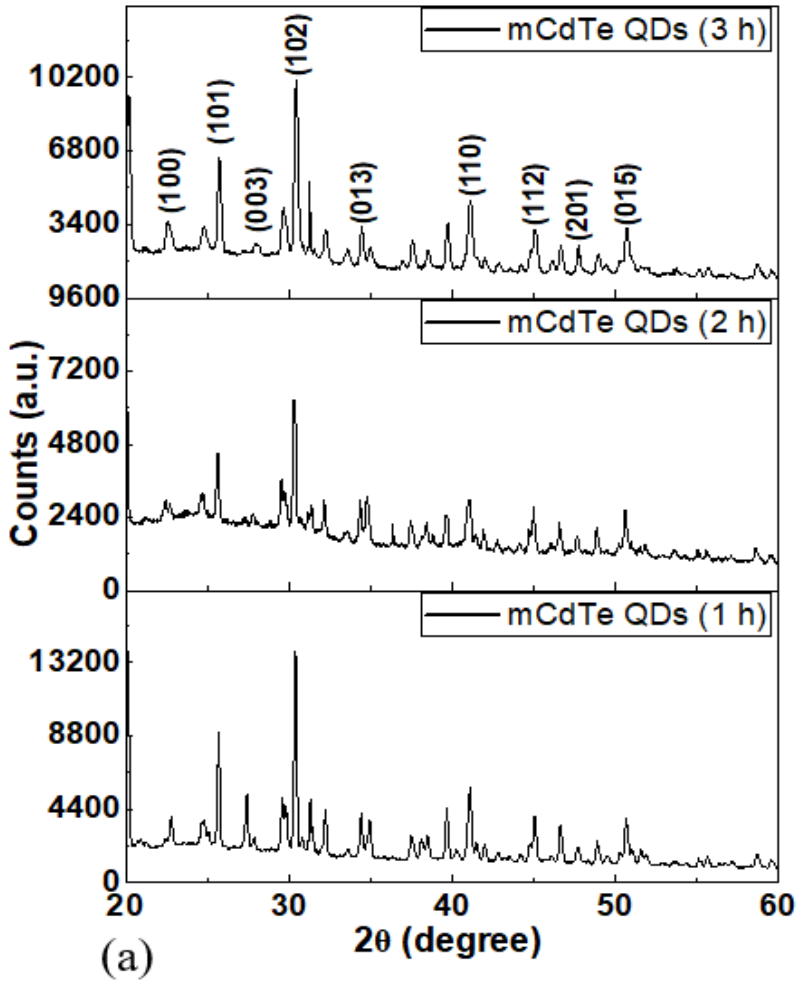

Peak list

No.	h	k	l	d [Å]	2θ [°]	I [%]
1	1	0	0	3.72478	23.870	7.6
2	1	0	1	3.50099	25.421	3.3
3	0	0	3	3.41833	26.046	0.1
4	1	0	2	3.01357	29.619	100.0
5	0	1	3	2.51851	35.619	0.9
6	1	1	0	2.15050	41.979	23.8
7	0	1	4	2.11185	42.784	32.7
8	1	1	1	2.10472	42.937	3.8
9	1	1	2	1.98314	45.713	8.2
10	2	0	0	1.86239	48.863	6.4
11	2	0	1	1.83242	49.716	0.7
12	1	1	3	1.82025	50.071	0.7
13	0	1	5	1.79664	50.776	0.4
14	0	2	2	1.75050	52.214	10.8
15	0	0	6	1.70917	53.575	5.3
16	1	1	4	1.64761	55.748	4.1
17	2	0	3	1.63542	56.200	1.9
18	1	0	6	1.55343	59.454	0.9
19	2	0	4	1.50678	61.491	5.9
20	1	1	5	1.48421	62.530	0.6
21	2	1	0	1.40783	66.344	2.1
22	1	2	1	1.39475	67.048	2.1
23	0	2	5	1.37878	67.929	0.2
24	1	0	7	1.36334	68.806	0.3
25	1	2	2	1.35759	69.138	8.6
26	1	1	6	1.33804	70.296	7.3
27	1	2	3	1.30175	72.561	0.4
28	2	0	6	1.25925	75.427	2.6
29	3	0	0	1.24159	76.693	1.0
30	2	1	4	1.23402	77.250	5.7
31	1	0	8	1.21210	78.915	3.6
32	3	0	2	1.20672	79.336	2.1
33	0	3	3	1.16700	82.610	0.7
34	2	1	5	1.16070	83.158	1.0
35	2	0	7	1.15145	83.977	0.1

(b)

Figure 2.

Edelweiss Applied Science and Technology
ISSN: 2576-8484
Vol. 10, No. 5: 238-256, 2026
DOI: 10.55214/2576-8484.v10i5.12913

(a) XRD pattern of mCdTe QDs refluxed at 1h, 2h, and 3 h, (b) JCPDS card.

By using the Debye-Scherrer formula, the average crystal sizes of the samples were estimated to be 0.375, 0.211, and 0.462 nm for 1, 2, and 3 hours refluxed samples, respectively [41]. The Debye-Scherrer formula is represented as:

$D = (0.89\lambda) / (\beta \cos \theta)$

where D is the mean crystal size, λ is the X-ray source wavelength (1.5404 Å), β is the full width at half maximum (FWHM), and θ is the diffraction angle of the respective peaks (Bragg's angle).

Nucleation and Ostwald ripening are the two prominent phenomena responsible for differences in the crystallite sizes of the samples [42, 43]. At 1 h, particle growth is still at the nucleation stage, resulting in large and poorly defined particles. By increasing the reflux time to 2 h, a steady growth rate is initiated, and particles become smaller and more compact. At this stage, growth is stabilized. Increasing the reflux time to 3 h causes enlargement of the particles as a result of close association and fusion of neighboring particles in a process known as Ostwald ripening [37].

4.1.3. Scanning Electron Microscopic (SEM) and Energy-Dispersive X-Ray Spectroscopy (EDX) Analysis

The SEM images of the synthesized nanomaterials are presented in Figures 3a-c for 1, 2, and 3 h-refluxed samples. The SEM images show clumped crystalline-like particles with a few distinct circular-shaped particles similar to those in literature [10]. The EDX spectra (Figures 3d-f) show Cd and Te as the major components of the samples, signifying successful mCdTe QDs production. The ratio of Cd and Te in the three samples (1 h, 0.54:0.46; 2 h, 0.58:0.42; 3 h, 0.51:0.49) varies, with the 2 h sample having the highest Cd content. Other elements present are sulfur, carbon, and oxygen, which come from the 3-mercaptopropionic acid ($C_3H_6O_2S$) used as the capping agent [44].

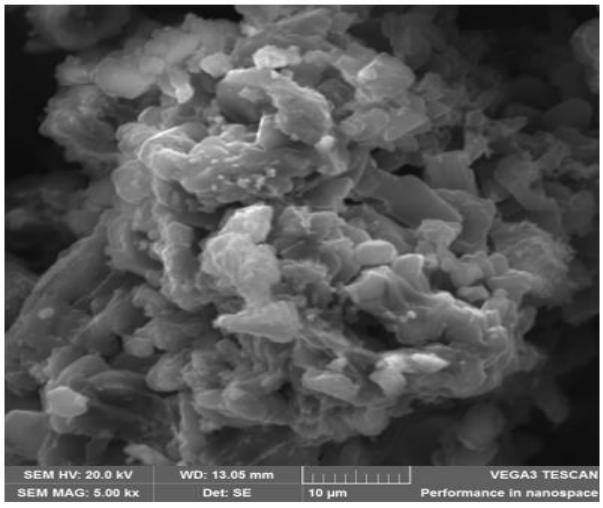

(a)

Edelweiss Applied Science and Technology
ISSN: 2576-8484
Vol. 10, No. 5: 238-256, 2026
DOI: 10.55214/2576-8484.v10i5.12913

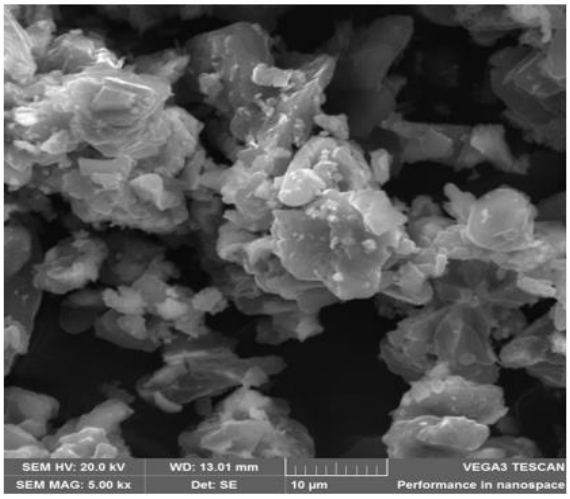

(b)

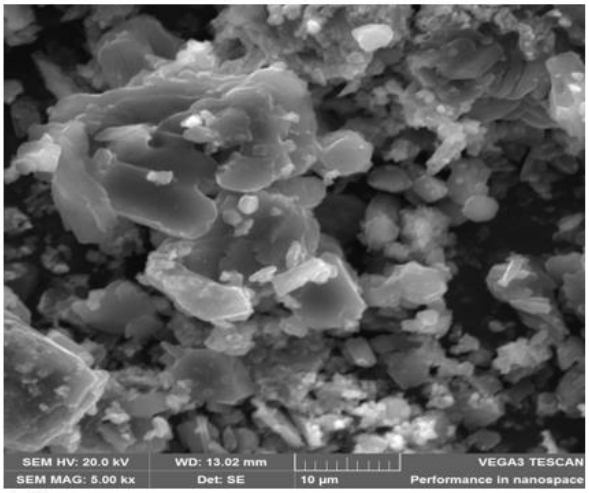

(c)

Edelweiss Applied Science and Technology
ISSN: 2576-8484
Vol. 10, No. 5: 238-256, 2026
***DOI**: 10.55214/2576-8484.v10i5.12913*

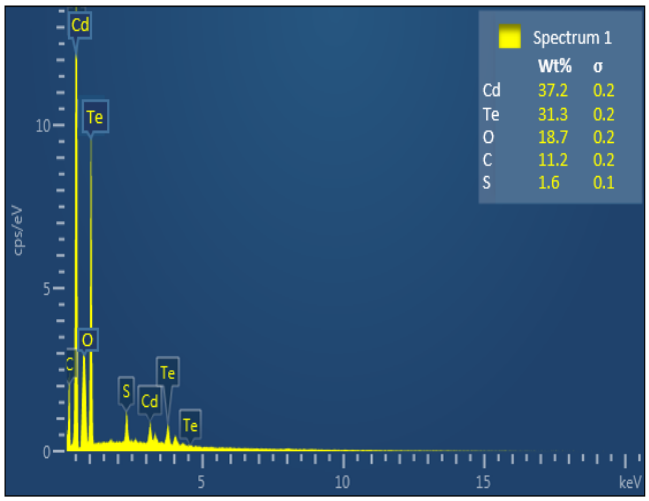

(d)

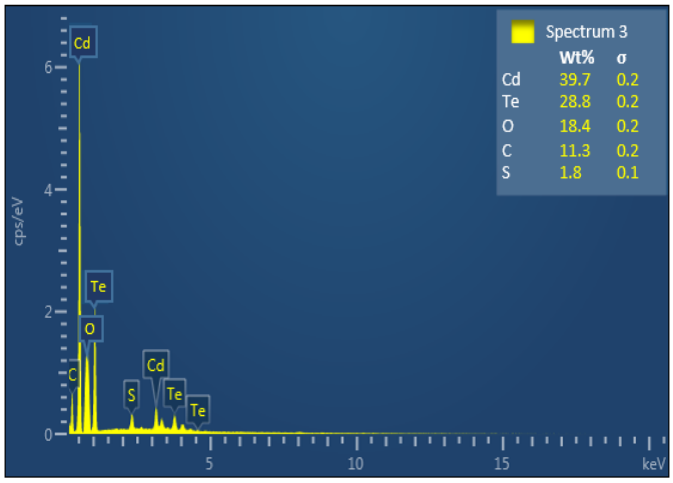

(e)

Edelweiss Applied Science and Technology
ISSN: 2576-8484
Vol. 10, No. 5: 238-256, 2026
DOI: 10.55214/2576-8484.v10i5.12913

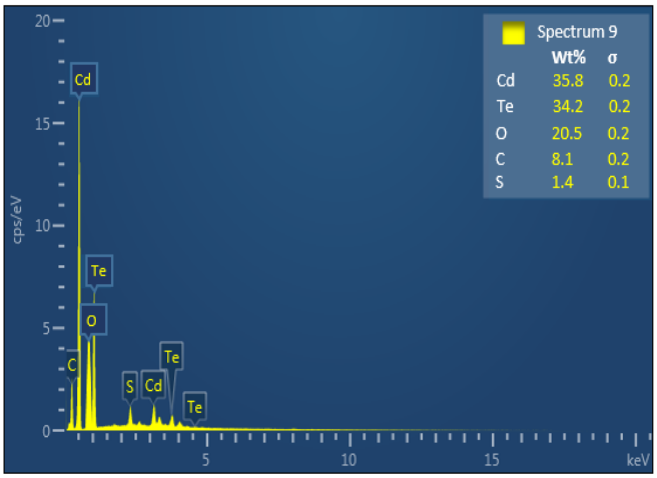

(f)

Figure 3.
SEM images of mCdTe QDs refluxed at a) 1 h, b) 2 h, c) 3 h and EDX spectra of mCdTe QDs refluxed at d) 1 h, e) 2 h, f) 3 h.

4.1.4. Transmission Electron Microscopy (TEM) Studies

Figures 4a-c represent the TEM micrographs of the synthesized mCdTe QDs at reflux times of 1, 2, and 3 hours, respectively. Distinct circular-shaped, uniformly distributed particles are observed across all 3 samples, with notable variations in average particle sizes. At a 1-hour reflux time, the average particle size was approximately 3.0 nm (Figure 4d). Increasing the reflux time to 2 hours decreased the particle size to about 2.7 nm (Figure 4e). Further extension of reflux to 3 hours resulted in a significant increase in average particle size to around 5.0 nm (Figure 4f). These differences in particle sizes are attributed to initial growth and incomplete nucleation in the 1-hour sample, enhanced crystallization, controlled nucleation, and stabilized particle growth at 2 hours, and Ostwald ripening due to extended particle growth at the expense of smaller particles in the 3-hour sample [45, 46]. Similar effects of reflux time on particle size have been reported in the literature [47].

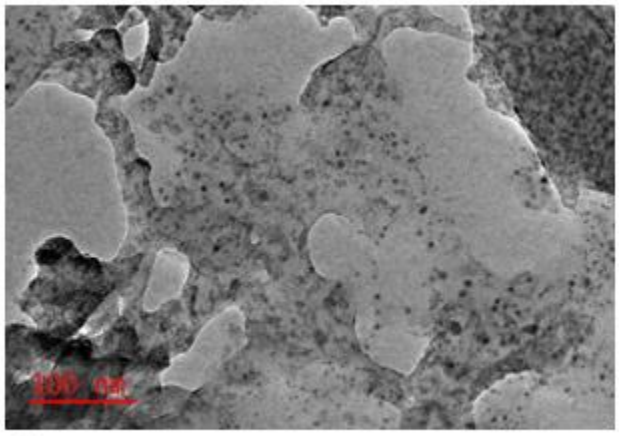

(a)

Edelweiss Applied Science and Technology
ISSN: 2576-8484
Vol. 10, No. 5: 238-256, 2026
DOI: 10.55214/2576-8484.v10i5.12913

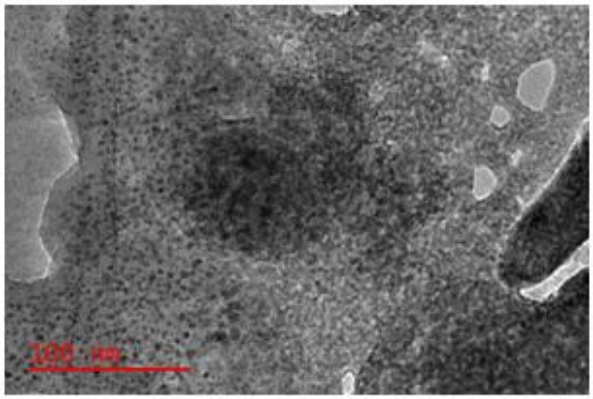

(b)

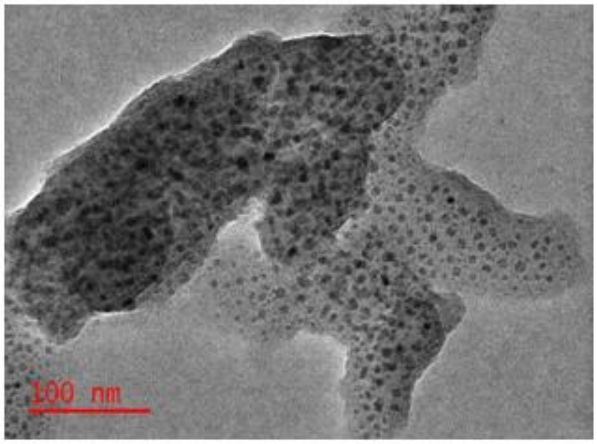

(c)

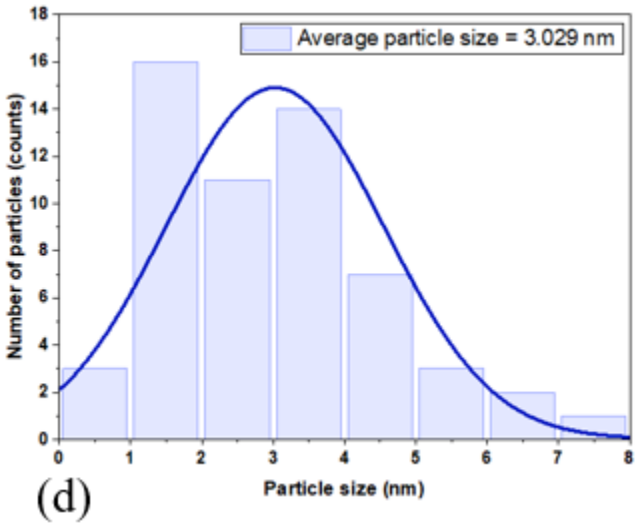

(d)

Edelweiss Applied Science and Technology
ISSN: 2576-8484
Vol. 10, No. 5: 238-256, 2026
DOI: 10.55214/2576-8484.v10i5.12913

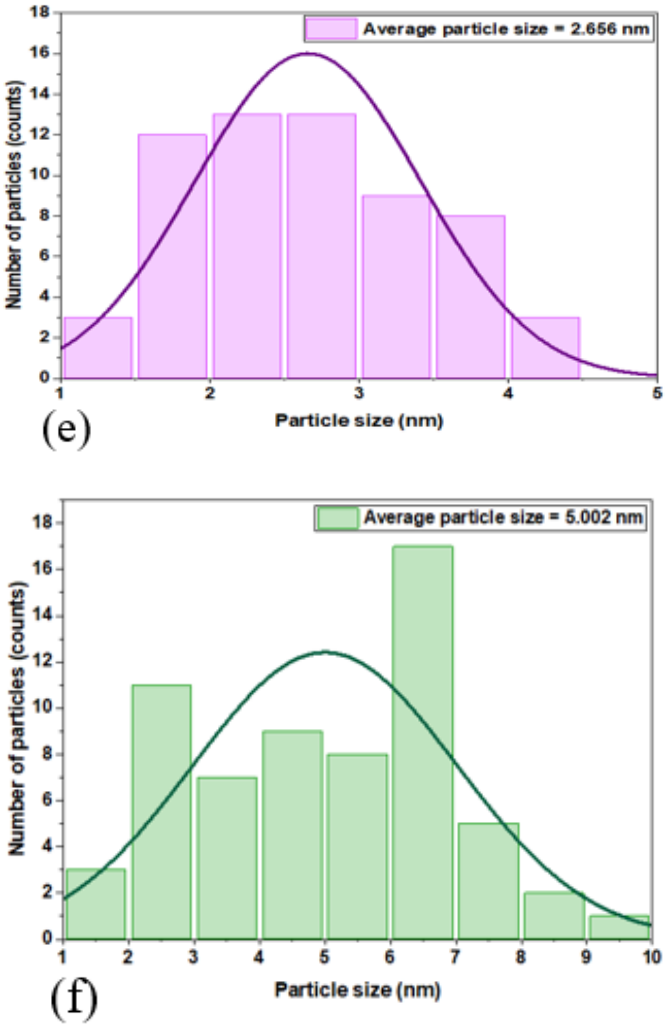

Figure 4.
TEM micrograph of mCdTe QDs refluxed at a) 1 h, b) 2 h, and c) 3 h, and their respective size distribution curve d) 1 h, e) 2 h, and f) 3 h.

4.2. Antibacterial Activity of mCdTe QDs

4.2.1. Agar Well Diffusion Assay

Results of the agar well diffusion study of mCdTe QDs against *Staphylococcus aureus* and *Escherichia coli* are presented in Figure 5. The clear zones (zones of inhibition) around the wells indicate the extent of microbial susceptibility to the quantum dots [26]. It clearly shows that the QDs have greater antimicrobial activity toward *E. coli* than *S. aureus*, with the 2 h refluxed sample having the widest zone of inhibition.

Edelweiss Applied Science and Technology
ISSN: 2576-8484
Vol. 10, No. 5: 238-256, 2026
DOI: 10.55214/2576-8484.v10i5.12913

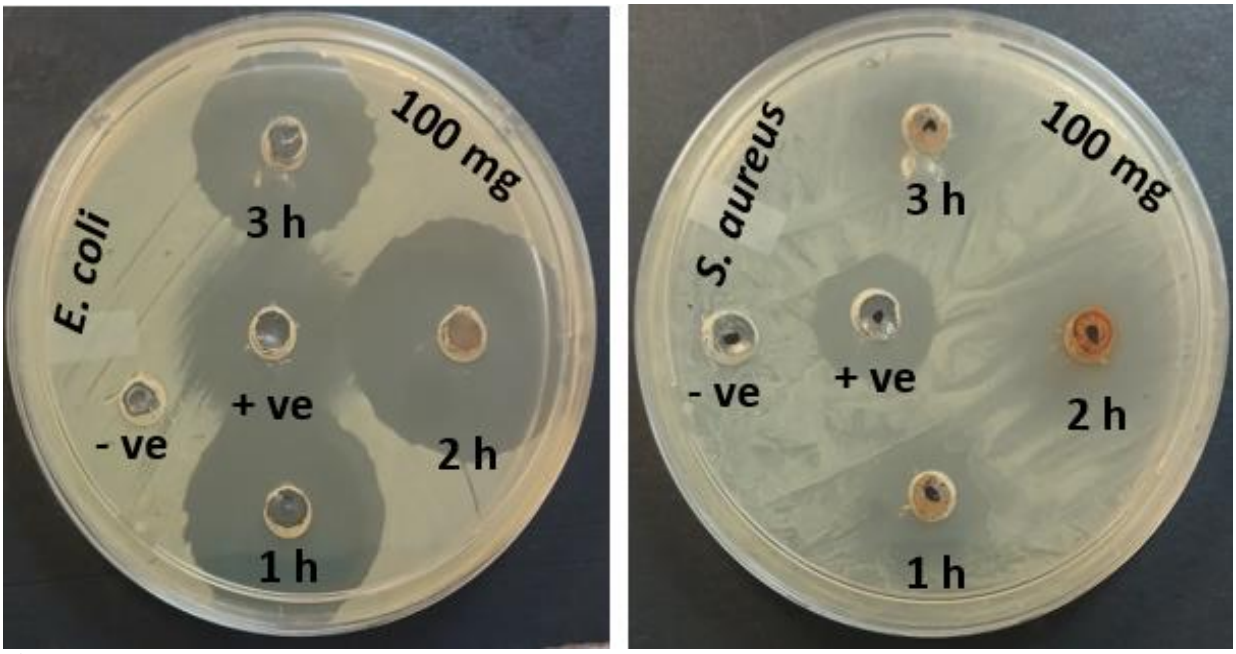

Figure 5.
Agar well diffusion assay for mCdTe QDs against *Escherichia coli* and *Staphylococcus aureus*. 1 h: 1-hour refluxing time; 2 h: 2 hours refluxing time; 3 h: 3 hours refluxing time; +ve: positive control (neomycin); -ve: negative control (milliQ water).

The diameter of the zones of inhibition was measured and recorded in Table 1. It shows that the synthesized nanomaterials exhibited antibacterial activity at all concentrations and refluxing times. The measurements show a dose-dependent pattern of antimicrobial activity. The higher the administered dose, the greater the antimicrobial activity. This is a common phenomenon with antimicrobial agents, as demonstrated in other works [1, 48]. Generally, the mCdTe QDs outperformed the standard antibiotics (neomycin) as an antimicrobial agent against both test organisms. The 2-hour refluxed sample has the biggest diameter of the zone of inhibition among the different tested concentrations. This superiority in activity over other samples refluxed at 1 and 3 hours is due to their smaller size (~2.7 nm; Figure 4e). The larger surface area-to-volume ratio enhances interaction with microbial cells and makes penetration of the nanomaterial easier [49, 50].

Table 1.
Zones of inhibition of mCdTe QDs at a concentration of 150 µg/ml in mm against test organisms.

Diameter of zones of inhibition (mm)										
Test Microorganisms	**mCdTe (mg/mL)**									**Neomycin**
	10			50			100			
	1h	2h	3h	1h	2h	3h	1h	2h	3h	
E. coli	24.3 ± 3.30	27.3 ± 1.70	22.7 ± 0.47	31.3 ± 0.94	34.7 ± 1.25	29 ± 0.82	33.0 ± 1.63	39.3 ± 1.25	31.7 ± 2.06	27.3 ± 1.89
S. aureus	16.7 ± 2.36	19.7 ± 2.06	12.3 ± 0.47	18.0 ± 0	22.3 ± 0.94	15.3 ± 0.47	20.3 ± 1.25	24.3 ± 0.47	19.0 ± 1.41	13.3 ± 1.35

4.2.2. Minimum Inhibitory (MIC) Test

The MIC assay is used to determine the lowest concentration of mCdTe QDs that inhibits bacterial growth [48]. Figure 6 shows the results of the MIC assay using a 96-well plate. Visual examination

Edelweiss Applied Science and Technology
ISSN: 2576-8484
Vol. 10, No. 5: 238-256, 2026
DOI: 10.55214/2576-8484.v10i5.12913

was used to determine the result by observing colour changes from blue to pink. This is because resazurin dye (blue), which is used as an indicator, is reduced to resorufin (pink) in the presence of viable bacterial cells, while the blue colour is retained where there are no viable cells [26]. The lowest concentration where no colour change was observed was noted and recorded as the MIC [1]. The results show that *E. coli* is more susceptible to mCdTe QDs and align with the agar well diffusion assay results (Table 1).

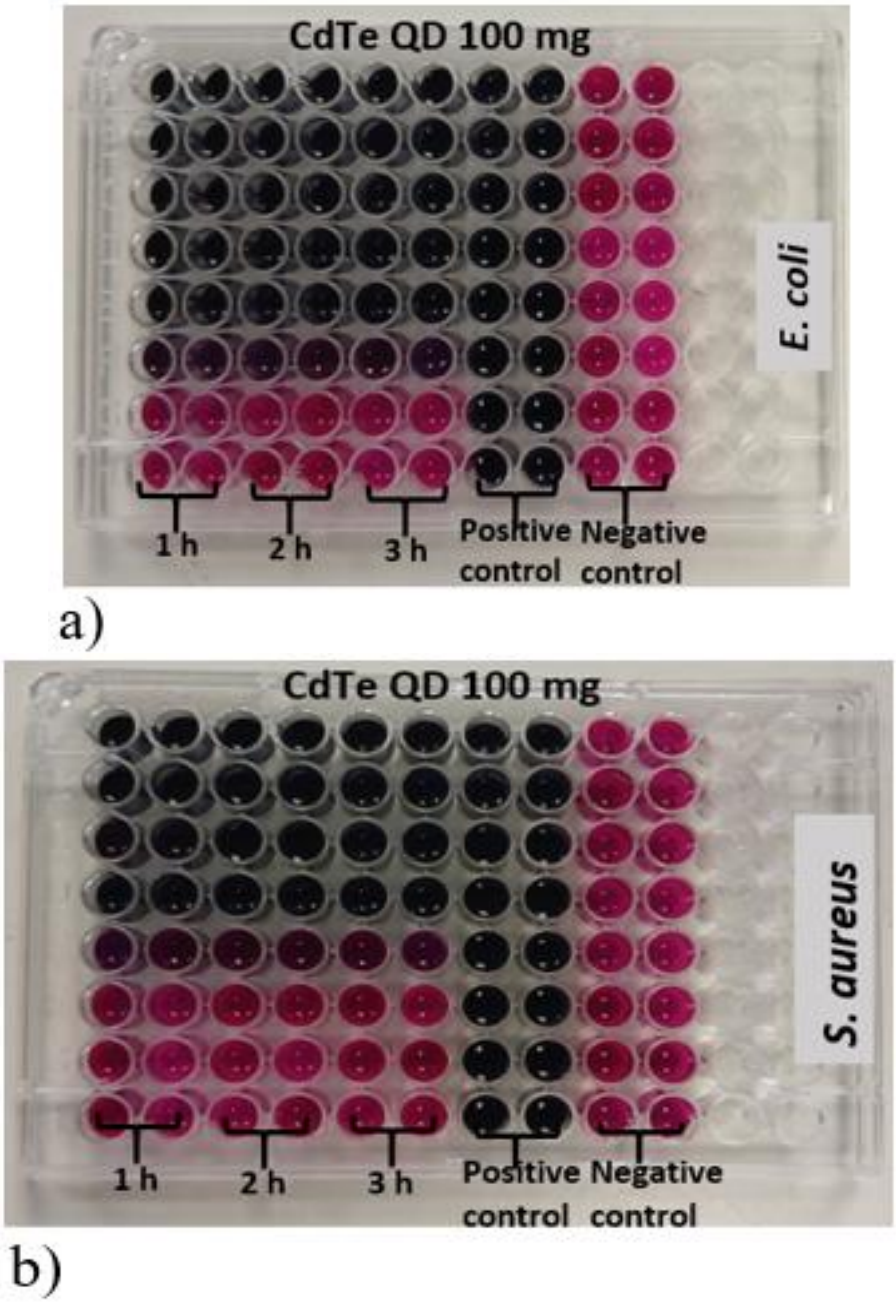

Figure 6.
Minimum inhibitory concentration test result for mCdTe QDs.

Edelweiss Applied Science and Technology
ISSN: 2576-8484
Vol. 10, No. 5: 238-256, 2026
DOI: 10.55214/2576-8484.v10i5.12913

Table 2 displays the MIC values of mCdTe QDs against *E. coli* and *S. aureus* at concentrations of 10, 50, and 100 mg/mL and at 1, 2, and 3 hours reflux times. For a fixed concentration, identical MIC values were observed across the various refluxing times for both test organisms. This indicates that varying the refluxing time during synthesis does not affect the inhibitory antimicrobial performance of mCdTe QDs. For neomycin, the MIC results show that it performed well as expected, but the associated antimicrobial resistance as a conventional antimicrobial agent remains a major setback [51].

Table 2.
Minimum inhibitory/bactericidal concentration test results for mCdTe QDs against test organisms.

MIC/ MBC											
Test Microorganisms		**mCdTe (mg/mL)**									**Neomycin (Positive control)**
		1 h			2 h			3 h			
		10	50	100	10	50	100	10	50	100	
E. coli	**MIC**	12.5	3.125	1.563	12.5	3.125	1.563	12.5	3.125	1.563	> 0.391
	MBC	NA	12.5	6.25	NA	6.25	3.125	NA	25	12.5	> 0.391
S. aureus	**MIC**	25	6.25	3.125	25	6.25	3.125	25	6.25	3.125	> 0.391
	MBC	NA	25	12.5	NA	12.5	6.25	NA	50	25	> 0.391

Note: MIC: minimum inhibitory concentration; MBC: minimum bactericidal concentration; NA: no activity.

4.2.3. Bactericidal Concentration (MBC) Test

Further antimicrobial examination of mCdTe QDs was conducted by determining the minimum bactericidal concentration, which is the lowest concentration of the nanomaterial capable of killing 99.9% of bacterial cells [27, 52]. The results, shown in Table 2, indicate that the bactericidal activity of the QDs depends on concentration, with 100 mg/mL exhibiting the highest activity. At 10 mg/mL, no bactericidal activity was observed for both E. coli and S. aureus at any refluxing time, rendering all samples bacteriostatic at this concentration. Among the samples, the 2-hour refluxed sample demonstrated the most bactericidal activity, followed by the 1-hour refluxed sample, with the 3-hour refluxed sample showing the least activity. This finding corroborates the agar well diffusion results (Table 1). The superior performance of the 2-hour sample is linked to its small particle size, which facilitates the easy entry of QDs into bacterial cells. Additionally, due to its lower crystallinity, as indicated by EDX studies, the 2-hour sample contains more defects, leading to increased ROS production and toxicity [53]. These results demonstrate that refluxing time significantly influences the antimicrobial activity of mCdTe QDs.

The antimicrobial activity of mCdTe QDs occurs through multiple pathways as shown in Figure 7: by the accumulation of the heavy metal ion Cd^{2+} within vesicle bodies, leading to cytotoxicity of the bacterial cell; or by exerting oxidative stress through downregulation of gene expression of the major antioxidant enzymes of the cell, which are superoxide dismutase and endonuclease IV; or through the anchoring of the QDs to the phospholipid bilayer at the lipophilic tail end, destroying the outer peptidoglycan layer of the cell wall [5].

Edelweiss Applied Science and Technology
ISSN: 2576-8484
Vol. 10, No. 5: 238-256, 2026
DOI: 10.55214/2576-8484.v10i5.12913

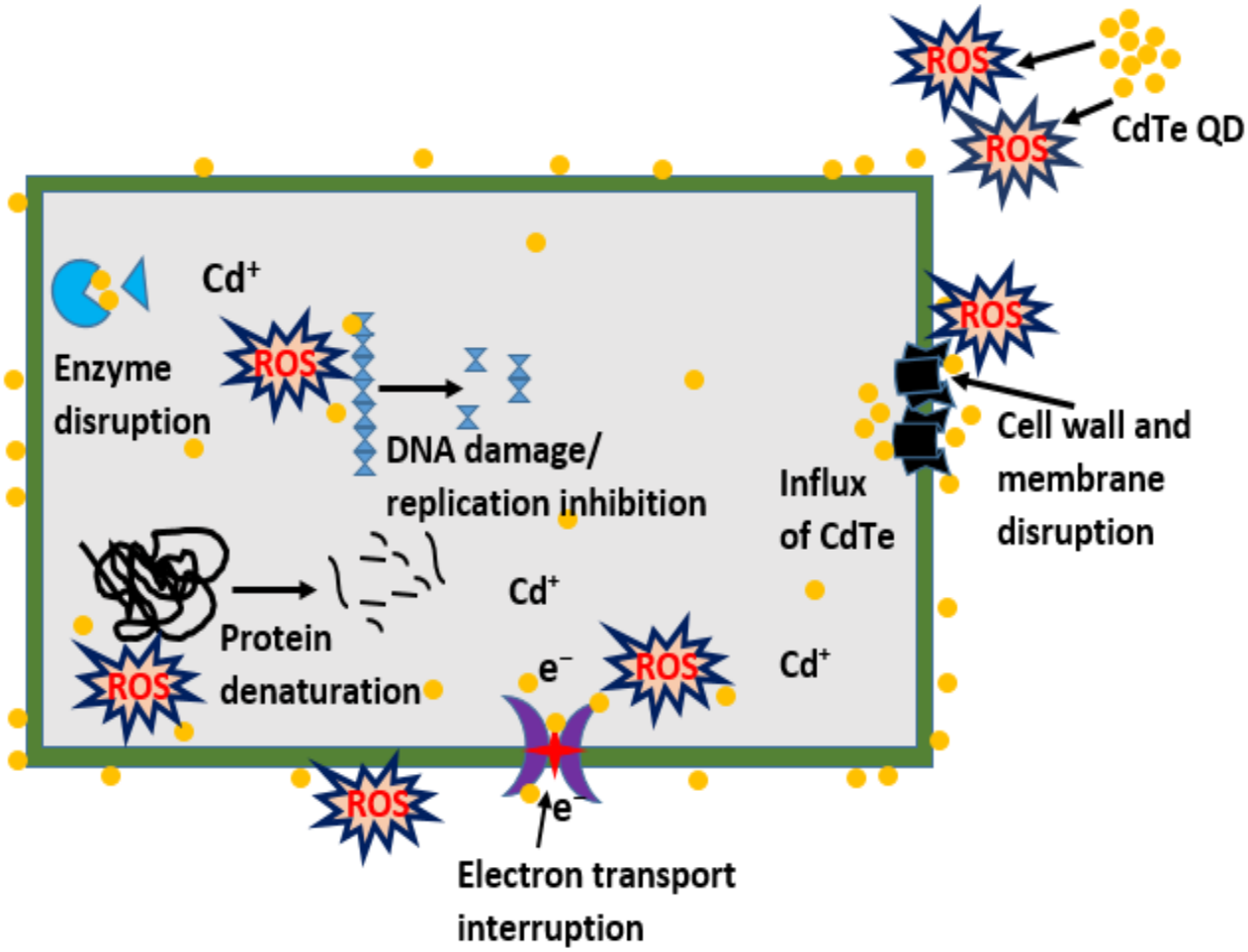

Figure 7.
Mechanism of antimicrobial activity of CdTe QDs.

The CdTe QDs, through a series of reactions, also generate reactive oxygen species (ROS), including hydrogen peroxide (H_2O_2), which can enter the cell and cause cell lysis [9, 50]. The increased susceptibility of E. coli to CdTe quantum dots is due to its gram-negative cell wall structure, which consists of a thin peptidoglycan layer and a lipopolysaccharide-containing outer membrane. Therefore, it easily allows the passage of the QDs, causing membrane damage more rapidly [50]. Conversely, *S. aureus* (gram-positive bacteria) has a thick peptidoglycan layer, providing better protection against environmental stress, hence the reduced antimicrobial activity.

4.3. Limitations of the Study

The safety of MPA-capped cadmium telluride quantum dots was not evaluated. Additionally, the antimicrobial activity of the quantum dots was assessed under ideal laboratory conditions, not in real or simulated biological environments. Therefore, further studies on biocompatibility and antimicrobial performance in physiologically relevant systems are essential to advance these nanomaterials toward practical biomedical applications.

Edelweiss Applied Science and Technology
ISSN: 2576-8484
Vol. 10, No. 5: 238-256, 2026
DOI: 10.55214/2576-8484.v10i5.12913

5. Conclusion

This study demonstrates the successful synthesis of 3-mercaptopropionic acid–capped cadmium telluride quantum dots (mCdTe QDs) under various refluxing times and establishes their promising antimicrobial potential against *Escherichia coli* and *Staphylococcus aureus*. Characterization of the quantum dots confirmed the formation of crystalline, nanoscale mCdTe QDs, with particle size strongly affected by refluxing time. Antimicrobial assessment showed a clear dose-dependent response, with the QDs exhibiting greater activity against *E. coli* than *S. aureus*, due to differences in their cell wall structures.

The 2 h refluxed CdTe QDs demonstrated superior antimicrobial performance among the samples, evidenced by their largest zones of inhibition and most pronounced bactericidal activity, due to their smaller particle size, higher surface area, and higher Cd^{2+} content. In contrast, MIC values remained consistent across refluxing times at identical concentrations, indicating that refluxing time primarily influences bactericidal rather than inhibitory activity. At 10 mg/mL, all samples exhibited bacteriostatic behavior against both test organisms, further emphasizing the concentration-dependent nature of their antimicrobial action.

The findings in this study highlight the importance of refluxing time as a synthesis parameter for optimizing the antibacterial performance of CdTe QDs. It also reinforces the potential of nanotechnology-based approaches as an alternative strategy to combat antimicrobial resistance.

Funding:

Support for this research was provided by Vaal University of Technology, Vanderbijlpark, South Africa.

Transparency:

The authors confirm that the manuscript is an honest, accurate, and transparent account of the study; that no vital features of the study have been omitted; and that any discrepancies from the study as planned have been explained. This study followed all ethical practices during writing.

References

[1] E. U. Ekwujuru, M. G. Peleyeju, C. Ssemakalu, M. Monapathi, and M. Klink, "Characterization and antimicrobial assessment of cadmium sulfide nanoparticles," *International Journal of Molecular Sciences*, vol. 27, no. 1, p. 432, 2025. https://doi.org/10.3390/ijms27010432

[2] A. J. Sabat, D. Pantano, V. Akkerboom, E. Bathoorn, and A. W. Friedrich, "Pseudomonas aeruginosa and Staphylococcus aureus virulence factors as biomarkers of infection," *Biological Chemistry*, vol. 402, no. 12, pp. 1565-1573, 2021. https://doi.org/10.1515/hsz-2021-0243

[3] C. Ghosh, P. Sarkar, R. Issa, and J. Haldar, "Alternatives to conventional antibiotics in the era of antimicrobial resistance," *Trends in Microbiology*, vol. 27, no. 4, pp. 323-338, 2019.

[4] C. L. de Dicastillo and M. G. Correa, "Dioxide Nanoparticles," *Antimicrobial Resistance: A One Health Perspective*, p. 95, 2021.

[5] K. Rajendiran, Z. Zhao, D. S. Pei, and A. Fu, "Antimicrobial activity and mechanism of functionalized quantum dots," *Polymers (Basel)*, vol. 11, no. 10, p. 1670, 2019. https://doi.org/10.3390/polym11101670

[6] T. Maxwell, M. G. N. Campos, S. Smith, M. Doomra, Z. Thwin, and S. Santra, *Quantum dots. In Nanoparticles for biomedical applications*. Amsterdam, Netherlands: Elsevier, 2020.

[7] S. Zhu *et al.*, "Photoluminescence mechanism in graphene quantum dots: Quantum confinement effect and surface/edge state," *Nano Today*, vol. 13, pp. 10-14, 2017. https://doi.org/10.1016/j.nantod.2016.12.006

[8] X. Chen, Z. Guo, and P. Miao, "One-pot synthesis of GSH-Capped CdTe quantum dots with excellent biocompatibility for direct cell imaging," *Heliyon*, vol. 4, no. 3, p. e00576, 2018. https://doi.org/10.1016/j.heliyon.2018.e00576

[9] B. Gidwani *et al.*, "Quantum dots: Prospectives, toxicity, advances and applications," *Journal of Drug Delivery Science and Technology*, vol. 61, p. 102308, 2021. https://doi.org/10.1016/j.jddst.2020.102308

[10] A. M. Kadim, *Applications of cadmium telluride (CdTe) in nanotechnology. In A. F. Simona Clichici & G. M. do Nascimento (Eds.), Nanomaterials—Toxicity, human health and environment.* London, United Kingdom: IntechOpen, 2019.

[11] C. M. Maguire *et al.*, "The anticoagulant properties of cadmium telluride quantum dots," *Journal of Interdisciplinary Nanomedicine*, vol. 3, no. 1, pp. 16-28, 2018. https://doi.org/10.1002/jin2.35

[12] Z. M. Alvand, H. R. Rajabi, A. Mirzaei, A. Masoumiasl, and H. Sadatfaraji, "Rapid and green synthesis of cadmium telluride quantum dots with low toxicity based on a plant-mediated approach after microwave and ultrasonic assisted extraction: Synthesis, characterization, biological potentials and comparison study," *Materials Science and Engineering: C*, vol. 98, pp. 535-544, 2019. https://doi.org/10.1016/j.msec.2019.01.010

[13] P. Modlitbová *et al.*, "Time-dependent growth of silica shells on CdTe quantum dots," *Nanomaterials*, vol. 8, no. 6, p. 439, 2018. https://doi.org/10.3390/nano8060439

[14] A. Kumari, S. K. Khare, and J. Kundu, "Adverse effect of CdTe quantum dots on the cell membrane of Bacillus subtilis: Insight from microscopy," *Nano-Structures & Nano-Objects*, vol. 12, pp. 19-26, 2017. https://doi.org/10.1016/j.nanoso.2017.08.003

[15] P. T. Wansapura, R. S. Dassanayake, A. Hamood, P. Tran, H. Moussa, and N. Abidi, "Preparation of chitin-CdTe quantum dots films and antibacterial effect on Staphylococcus aureus and Pseudomonas aeruginosa," *Journal of Applied Polymer Science*, vol. 134, no. 22, 2017. https://doi.org/10.1002/app.44904

[16] B. Poormoradi, S. Dehghani, H. Zare, M. Y. Alikhani, J. M. Haghgoo, and A. Farmany, "Enhanced antibacterial activity of cadmium telluride nanocrystals in combination with 940-nm laser diode on anaerobic bacteria P. gingivalis: an in vitro study," *Lasers in Medical Science*, vol. 38, p. 112, 2023. https://doi.org/10.1007/s10103-023-03773-7

[17] E. Gharibshahi, "Simulation, synthesis and optical properties of cadmium telluride (CdTe) semiconductor nanoparticles," *Solid State Communications*, vol. 320, p. 114009, 2020. https://doi.org/10.1016/j.ssc.2020.114009

[18] R. Aguilar-Garay *et al.*, "A comprehensive review of silver and gold nanoparticles as effective antibacterial agents," *Pharmaceuticals*, vol. 17, no. 9, p. 1134, 2024. https://doi.org/10.3390/ph17091134

[19] N. Zubair and K. Akhtar, "Morphology controlled synthesis of ZnO nanoparticles for in-vitro evaluation of antibacterial activity," *Transactions of Nonferrous Metals Society of China*, vol. 30, no. 6, pp. 1605-1614, 2020. https://doi.org/10.1016/S1003-6326(20)65323-7

[20] M. S. Giroux, Z. Zahra, O. A. Salawu, R. M. Burgess, K. T. Ho, and A. S. Adeleye, "Assessing the environmental effects related to quantum dot structure, function, synthesis and exposure," *Environmental Science: Nano*, vol. 9, no. 3, pp. 867-910, 2022. https://doi.org/10.1039/D1EN00712B

[21] F. F. Sead *et al.*, "Electrochemical behavior of carbon quantum dots as electrolyte additives for enhanced battery and supercapacitor performance," *Materials Technology*, vol. 40, no. 1, p. 2500524, 2025. https://doi.org/10.1080/10667857.2025.2500524

[22] A. Girma, G. Mebratie, B. Mekuye, B. Abera, T. Bekele, and G. Alamnie, "Antibacterial capabilities of metallic nanoparticles and influencing factors," *Nano Select*, vol. 5, no. 12, p. e202400049, 2024. https://doi.org/10.1002/nano.202400049

[23] L. Wang, C. Hu, and L. Shao, "The antimicrobial activity of nanoparticles: Present situation and prospects for the future," *International Journal of Nanomedicine*, vol. 12, pp. 1227-1249, 2017. https://doi.org/10.2147/IJN.S121956

[24] Y. Shan, J.-J. Xu, and H.-Y. Chen, "Electrochemiluminescence quenching by CdTe quantum dots through energy scavenging for ultrasensitive detection of antigen," *Chemical Communications*, vol. 46, no. 28, pp. 5079-5081, 2010. https://doi.org/10.1039/C0CC00837K

[25] G. Lanza, J. A. Perez-Taborda, and A. Avila, "Improving temperature adaptation for food safety: Colorimetric nanoparticle-based time–temperature indicators (TTIs) to detect cumulative temperature disturbances," *Foods*, vol. 14, no. 5, p. 742, 2025. https://doi.org/10.3390/foods14050742

[26] G. Moukangoe *et al.*, "Synthesis and antibacterial activity of Cobalt-thiourea nanoparticles on selected waterborne bacterial pathogens," *Digest Journal of Nanomaterials and Biostructures*, vol. 15, pp. 757-766, 2020.

Edelweiss Applied Science and Technology
ISSN: 2576-8484
Vol. 10, No. 5: 238-256, 2026
DOI: 10.55214/2576-8484.v10i5.12913

[27] P. Parvekar, J. Palaskar, S. Metgud, R. Maria, and S. Dutta, "The minimum inhibitory concentration (MIC) and minimum bactericidal concentration (MBC) of silver nanoparticles against Staphylococcus aureus," *Biomaterial Investigations in Dentistry*, vol. 7, no. 1, pp. 105-109, 2020. https://doi.org/10.1080/26415275.2020.1796674

[28] A. Azam, A. S. Ahmed, M. Oves, M. S. Khan, S. S. Habib, and A. Memic, "Antimicrobial activity of metal oxide nanoparticles against Gram-positive and Gram-negative bacteria: A comparative study," *International Journal of Nanomedicine*, vol. 7, pp. 6003-6009, 2012. https://doi.org/10.2147/IJN.S35347

[29] D. B. Howard and B. K. Harvey, "Assaying the stability and inactivation of AAV serotype 1 vectors," *Human Gene Therapy Methods*, vol. 28, no. 1, pp. 39-48, 2017. https://doi.org/10.1089/hgtb.2016.180

[30] C. Zhao *et al.*, "High-throughput gene replacement in Aspergillus fumigatus," *Current Protocols in Microbiology*, vol. 54, no. 1, p. e88, 2019. https://doi.org/10.1002/cpmc.88

[31] R. Hulankova, "Methods for determination of antimicrobial activity of essential oils in vitro—a review," *Plants*, vol. 13, no. 19, p. 2784, 2024. https://doi.org/10.3390/plants13192784

[32] Z. Montaseri, A. M. Tamaddon, M. J. Raee, and F. Farvadi, "Exploring the effects of various capping agents on zinc sulfide quantum dot characteristics and in-vitro fate," *ChemistryOpen*, vol. 12, no. 10, p. e202300094, 2023. https://doi.org/10.1002/open.202300094

[33] M. B. Nayan, K. Jagadish, M. R. Abhilash, K. Namratha, and S. Srikantaswamy, "Comparative study on the effects of surface area, conduction band and valence band positions on the photocatalytic activity of ZnO-M x O y heterostructures," *Journal of Water Resource and Protection*, vol. 11, no. 03, p. 357, 2019.

[34] R. Martin-Trasanco *et al.*, "In-situ preparation of CdTe quantum dots capped with a β-cyclodextrin-epichlorohydrin polymer: Polymer influence on the nanocrystal's optical properties," *Nanomaterials*, vol. 8, no. 11, p. 948, 2018. https://doi.org/10.3390/nano8110948

[35] S. Somathube, O. A. Daramola, P. B. Lokole, J. B. Safari, X. Siwe-Noundou, and F. B. Dejene, "Synthesis of ZnSe QDs: Effects of stabilizer on the optical properties and structural morphology," *Results in Physics*, vol. 73, p. 108262, 2025. https://doi.org/10.1016/j.rinp.2025.108262

[36] S. Surabhi, K. Anurag, and S. Kumar, "Effect of annealing on the structural, compositional and optical properties of CdTe films," *Materials Today: Proceedings*, vol. 45, pp. 4477-4482, 2021. https://doi.org/10.1016/j.matpr.2020.12.988

[37] H. N. Noori and A. F. Abdulameer, "Study of optical and structural properties of CdTe quantum dots capped with 3MPA using hydrothermal method," *Chemical Methodologies*, vol. 6, no. 11, pp. 842-850, 2022.

[38] G. Sindhu, M. Manikandan, S. Dhanuskodi, and M. A. Arasu, "One-pot synthesis of MPA capped CdTe quantum dots for non-enzymatic hydrogen peroxide biosensor application," *International Journal of Scientific Research in Science and Technology*, vol. 3, pp. 129-134, 2017.

[39] A. F. Butt *et al.*, "Chemically processed CdTe thin films for potential applications in solar cells–Effect of Cu doping," *Heliyon*, vol. 10, no. 3, p. e24492, 2024.

[40] N. Putra, Sugianto, B. Astuti, and P. Marwoto, "Absorber performation of CdTe/CdTe: Cu thins films based from crystal phase and microstructures," in *ournal of Physics: Conference Series (Vol. 1321, No. 2, p. 022018). IOP Publishing*, 2019.

[41] C. Ragupathi *et al.*, "Correlation between the particle size, structural and photoluminescence spectra of nano NiCr(2)O(4) and La doped NiCr(2)O(4) materials," *Heliyon*, vol. 9, no. 11, p. e21981, 2023. https://doi.org/10.1016/j.heliyon.2023.e21981

[42] H. Wasly, M. A. El-Sadek, and M. Henini, "Influence of reaction time and synthesis temperature on the physical properties of ZnO nanoparticles synthesized by the hydrothermal method," *Applied Physics A*, vol. 124, no. 1, p. 76, 2018. https://doi.org/10.1007/s00339-017-1482-4

[43] S. Bandyopadhyay and S. Ucar, "Nucleation and growth of nanoparticles," *Engineering Nanoparticles for Biomedical Applications: From Theory to Experiments and Modeling*, pp. 1-21, 2026.

[44] M. Mrad *et al.*, "Aqueous synthesis for highly emissive 3-mercaptopropionic acid-capped AIZS quantum dots," *Inorganic Chemistry*, vol. 59, no. 9, pp. 6220-6231, 2020. https://doi.org/10.1021/acs.inorgchem.0c00347

[45] A. Priyam, A. Chatterjee, S. C. Bhattacharya, and A. Saha, "Surface-functionalized cadmium chalcogenide nanocrystals: A spectroscopic investigation of growth and photoluminescence," *Journal of Crystal Growth*, vol. 304, no. 2, pp. 416-424, 2007. https://doi.org/10.1016/j.jcrysgro.2007.02.026

[46] S. Reja, M. Kumar, and S. Vasudevan, "Low-cost one-pot synthesis of hydrophobic and hydrophilic monodispersed iron oxide nanoparticles," *Nanoscale Advances*, vol. 6, no. 15, pp. 3857-3864, 2024.

[47] Z. Akram, M. Qasim, S. Riaz, and S. Naseem, "Synthesis and characterization of CdTe ink comprised of nanoparticles," in *The 2012 World Congress on Advances in Civil, Environmental, and Materials Research, ACEM*, 2012.

[48] H. Mohd Yusof, N. A. Abdul Rahman, R. Mohamad, U. Hasanah Zaidan, and A. A. Samsudin, "Antibacterial potential of biosynthesized zinc oxide nanoparticles against poultry-associated foodborne pathogens: An in vitro study," *Animals*, vol. 11, no. 7, p. 2093, 2021. https://doi.org/10.3390/ani11072093

[49] V. A. Ershov and B. G. Ershov, "Effect of silver nanoparticle size on antibacterial activity," *Toxics*, vol. 12, no. 11, p. 801, 2024. https://doi.org/10.3390/toxics12110801

[50] B. Lallo da Silva *et al.*, "Relationship between structure and antimicrobial activity of zinc oxide nanoparticles: An overview," *International Journal of Nanomedicine*, vol. 14, pp. 9395-9410, 2019.

[51] I. Berger and Z. G. Loewy, "Antimicrobial resistance and novel alternative approaches to conventional antibiotics," *Bacteria*, vol. 3, no. 3, pp. 171-182, 2024. https://doi.org/10.3390/bacteria3030012

[52] S. Jaiswal and P. Mishra, "Antimicrobial and antibiofilm activity of curcumin-silver nanoparticles with improved stability and selective toxicity to bacteria over mammalian cells," *Medical Microbiology and Immunology*, vol. 207, no. 1, pp. 39-53, 2018. https://doi.org/10.1007/s00430-017-0525-y

[53] I. Perelshtein, A. Lipovsky, N. Perkas, A. Gedanken, E. Moschini, and P. Mantecca, "The influence of the crystalline nature of nano-metal oxides on their antibacterial and toxicity properties," *Nano Research*, vol. 8, pp. 695-707, 2015. https://doi.org/10.1007/s12274-014-0553-5

Edelweiss Applied Science and Technology
ISSN: 2576-8484
Vol. 10, No. 5: 238-256, 2026
DOI: 10.55214/2576-8484.v10i5.12913